INTERNATIONAL
Agrophysics
www.international-agrophysics.org

Int. Agrophys., 2013, 27, 409-417
doi: 10.2478/intag-2013-0011

Using satellite data for soil cation exchange capacity studies

M. Ghaemi[1], *A.R. Astaraei*[1], *S.H. Sanaeinejad*[2], *and H. Zare*[3]

[1]Department of Soil Science, [2]Department of Water Engineering, [3]Department of Agronomy, Ferdowsi University of Mashhad, FUM Campus, Azadi Sq., Mashhad, Khorasan Razavi, Iran

Received July 31, 2012; accepted October 29, 2012

A b s t r a c t. This study was planned to examine the use of LandSat ETM^+ images to develop a model for monitoring spatial variability of soil cation exchange capacity in a semi-arid area of Neyshaboor. 300 field data were collected from specific GPS registered points, 277 of which were error free, to be analysed in the soil laboratory. The statistical analysis showed that there was a small R-Squared value, 0.17, when we used the whole data set. Visual interpretation of the graphs showed a trend among some of the data in the data set. Forty points were filtered based on the trends, and the statistical analysis was repeated for those data. It was discovered that the 40 series were more or less in the same environmental conditions; most of them were located in disturbed soils or abandoned lands with sparse vegetation cover. The soil was classified into high and medium salinity, with variable carbon (1.0 to 1.6%), heavy textured and with high silt and clay. Finally it was concluded that two different models could be fitted in the data based on their spatial dependency. The current models are able to explain spatial variability in almost 45 to 65% of the cases.

K e y w o r d s: soil cation exchange capacity, remote sensing, soil properties, soil spatial variability

INTRODUCTION

Using remote sensing technology often reduces costs and increases accuracy and speed. By using remote sensing data three main categories of information are recognised: soil properties based on its reflectance band and the resulting images, the effect of soil surface conditions on the reflected radiation, and the simulated patterns which can be used for producing maps of soil variability (Johannsen *et al*., 1998).

The most comprehensive and detailed geographical world soil resources are presented in the global soil map in the scale of 1:5 000 000. This map is an integrated national and regional map based on a common legend. It contains different information including available water capacity, soil organic carbon content, soil pH, soils cation exchange capacity (CEC), soil drainage classes, soil depth classes and so on. The density and quality of available profiles is dramatically variable from one area to another (Batjes, 2002).

Different studies show that the relationship between satellite data and soil characteristics is more clear in 3.0 to 8.2 μm. Spectral response in this band is due to differences in organic matter content, iron levels, soil moisture and soil texture. The highest correlation with soil characteristics derived from the reflected bands data is known as albedo (Post *et al*., 2000).

In the saline area, most of the signal strengths are related to soluble salt concentration, while in non-saline soil, EC variability of soil is a function of organic matter content, soil texture, soil moisture and soil cation exchange capacity (Barnes *et al*., 2003).

Matinfar *et al*. (2011) used ASTER sensor data in order to study soils, and their results showed soils which have soft and dark uneven surfaces that are well separated in visible and thermal wave.

Fox and Metla (2005) took three types of soil line and used PCA (Principal component analysis) and regression analysis to assess soil characteristics, including soil organic carbon and exchange capacity. Those were compared and showed that PCA with high correlation (R^2= 0.32) gave better results for describing soil characteristics changes than the other two analysis methods. The researchers suggested that PCA could be used as a method of sampling in determining location of soil samples compared to the soil line model.

Remote sensing technology has a high potential for the characterisation of the spatial variation of soil properties at large scales, so this approach can provide valuable information for application to precision agriculture and environmental

*Corresponding author e-mail: ghaemi27@gmail.com

modelling. According to this goal, we explored the possibility of using digital analysis of satellite data and also multivariate regression analysis between cation exchange capacity and image data to find the best model for monitoring and study of soil in arid and semi-arid areas. The potential of ETM^+ images for studying cation exchange capacity in soil was also investigated.

MATERIAL AND METHODS

The study area was located in the Neyshaboor plain in Khorasan-Razavi province in the N-E of Iran, geographically located between longitudes 58.57 to 59.13° and latitudes 35.85 to 36.25° (Fig. 1). The climate is arid to semi-arid, with annual average temperature of 14.5°C and precipitation of 250 mm based on Ambergeh climate classification method. According to land-use maps, this area is generally saline with agricultural activities.

LandSat ETM^+ images including 6 bands with 30 m resolution, one thermal band with 60 m resolution and a panchromatic band with 15 m resolution, from track 160 and row 35, taken on 10th of July 2002, were used. The images were originally corrected for general geometric and radiometric errors.

However, more geometric corrections were also applied for more confidence. Various image processing techniques were used, including image enhancement, PCA, tasseled cap transformation, and also 50 vegetation and soil indices derived from the images. Some of the indices are listed in Table 1.

The ETM^+ images were converted into an appropriate format to be used in ERDAS Imagine 8.6 and IDRISI Kilimanjaro software.

After pre-processing of the images, their general features were compared with the corresponding land use map (scale: 1:250 000). A part of Neyshaboor plain with 765 km^2 was selected based on soil properties and vegetation cover estimated from field observations. That area is contained in an area of 1 881×1 497 pixels in the image. The area was divided into three main parts depending on their salinity determined from land use map and field observations. A grid with 10×50 mesh was drawn, with 1 000 m grid length on the area (Fig. 2). 100 of the grid cells were randomly selected and 3 separate points 100 m apart were chosen in each selected cell as sampling points. A sample of soil (20×20 cm surface and 20 cm depth) was recovered from each sampling point. The geographic position was recorded by a Garmin GPS and the samples were transported to a soil laboratory for testing.

The recovered soil samples were air dried and then sieved through a 2 mm sieve for laboratory testing. Different parameters were measured, including soil acidity by using a pH meter, EC in soil saturation extracts by an EC meter, soil organic carbon (SOC) by Walkely and Black (1934) method, cation exchange capacity (CEC) by Chapman (1965) method, and soil particle size distribution was determined by standard hydrometer method (Gee and Bauder, 1986).

JMP4 software was used for the statistical analysis. The derived R-Squares from regression analysis between soil cation exchange capacity values and the values of spectral satellite image were evaluated. Then the most appropriate independent variables were selected to estimate the dependent variables based on a multivariate linear regression (stepwise regression) equation. All the coefficients were considered statistically significant at 95% confidence level.

RESULTS AND DISCUSSION

The R-Square was low when all of the data from the low to high salinity soil samples were considered in the regression analysis (Table 2). The highest R-squares were obtained between the main bands, including bands 1, 2 and 3, the amounts for which were 0.06 0.04 and 0.1, respectively. Indices (PD311 = TM3-TM2), (PD321 =TM3-TM1), BI1, SI showed a higher correlation. Appropriate model for achieving stepwise regression method was applied and the variables with the highest R-square were used to obtain Eq. (1) for the total data set.

$$\text{CEC}= 9.6+4.09\ \text{PD321}+3.3\ \text{PD311}+0.08\ \text{b3}\ . \qquad (1)$$

In this equation, CEC is cation exchange capacity in meq 100 g^{-1} with R-square=0.17 and RMSE = 4.22. Regression analysis data for the whole range of the data set, in which the non-saline and saline soils are included, showed very low R-squares. The results of regression analysis, statistically significant at 5% level, showed that Eq. (1) could not provide a good estimate for CEC. Obviously, this equation with low RMSE coefficient does not have a high R-square. Phillips (1994) in his research showed that R-squared values of 0.2 to 0.5 can show comprehensive information for soil studies in large scale studies. It is not possible to have a correct assess of the cation exchange capacity for the region if this equation with the obtained R-square for the entire data is used. It should be noted that other researchers like Dematte *et al*. (2007) also reported weak correlations between some soil chemical properties such as Ca, Mg, Al, pH and K values in soil. Although, the correlation coefficient was between 0.3 and 0.4 when organic matter, sand and clay percentage were considered for the analysis. Accordingly, the distribution diagrams were studied closely and it was observed that some parts of the process are different than others (Fig. 3). The points with different digital values were classified and soil properties were analysed separately in each class (Fig. 4).

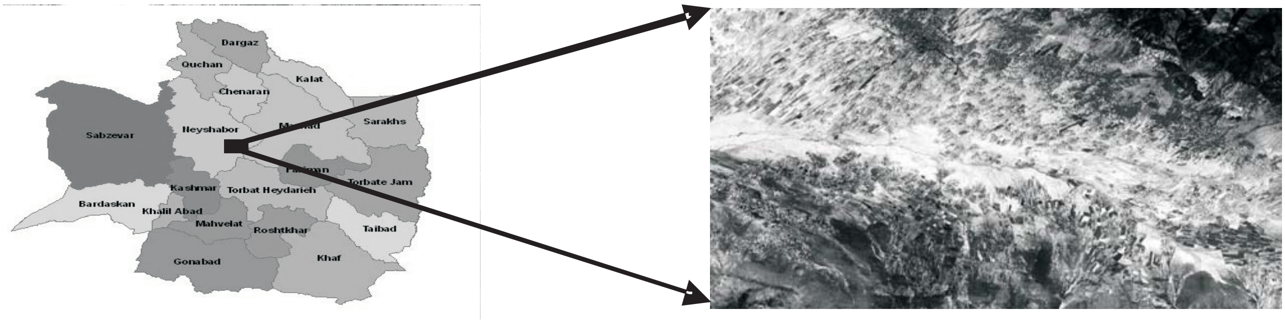

Fig. 1. Geographical location of the study area.

T a b l e 1. Some of the principal and artificial bands used in this research

Index name	Equation	Reference
Near Inferared Ratio (NIR)	TM4/TM3	Pettorelli *et al*., 2005
Leaf Water Content(Mid-IR-Index)	TM5/TM7	Pettorelli *et al*., 2005
Normalized Difference Vegetation Index	(TM4-TM3)/(TM4+TM3)	Foody *et al*., 2001
Transformed Vegetation Index	(TM5-TM3)/(TM5+TM3)	Pettorelli *et al*., 2005
Reflectance Absorption Index	TM4/(TM3+TM5)	Arzani and King, 2008
Modified Normalized Difference	(TM4-(1.2×TM3)/(TM4+TM3)	Pettorelli *et al*., 2005
PD321	TM3-TM2	Arzani and King, 2008
PD311	TM3-TM1	Arzani and King, 2008
MIRV1	(TM7-TM3)/(TM7+TM3)	Leblon, 1993
DVI	TM4-TM3	Foody *et al*., 2001
MIRV2	(TM5-TM3)/(TM5-TM3)	Arzani and King, 2008
Green Vegetation Index	-0.29 (G) -0.56(R)+0.6(IR)+0.49(IR)	Leblon, 1993
SAVI	[NIR-RED)/(NIR+RED+L)] × (1+L)	Pettorelli *et al*., 2005
GEMI	η× (1-0.25×η)-(Red-0.125) / (1-Red)	Nikolakopoulos , 2003
OSAVI	(NIR -Red) / (NIR + Red + 0.16)	Nikolakopoulos , 2003
Stress-related	(TM1×TM2)/TM3	Foody *et al*., 2001
Normalized-based	(TM4 - (TM1 + TM2))/(TM4 + (TM1 + TM2))	Foody *et al*., 2001
PCA1	Derived from principal components of bands 1, 2 and 3	Bahtti *et al*., 1991; Frazier and Cheng, 1989
PCA2	Derived from principal components of bands 4, 5 and 7	Bahtti *et al*., 1991; Frazier and Cheng, 1989
PCA3	Derived from principal components of bands 1,2, 3, 5, 7 and 4	Bahtti *et al*., 1991; Frazier and Cheng, 1989
Brightness	Brightness derived from tasseled cap	Bahtti *et al*., 1991; Frazier and Cheng, 1989
Greenness	Greeness band derived from tasseled cap	Bahtti *et al*., 1991; Frazier and Cheng, 1989
Wetness	Humid bands derived from tasseled cap	Bahtti *et al*., 1991; Frazier and Cheng, 1989

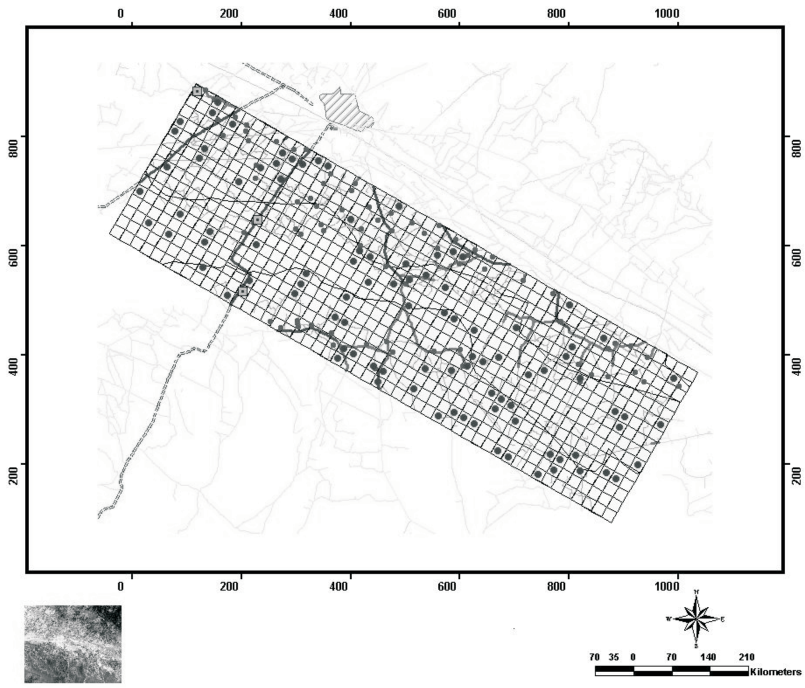

Fig. 2. Position of random locations for sampling points.

The results showed that the 40 series were located in degraded and abandoned agricultural lands with scattered vegetation cover. The areas contain moderate to high salinity lands in the area. Organic carbon in these parts is variable between 1 and 1.6%. Total amounts of silt and clay in these lands are high and heavy textured soils are included (Fig. 5). This shows that high levels of organic carbon in the low density vegetation areas (due to destruction of vegetation) are affected by the amount of cation exchange capacity and percentage of clay, especially high electrical conductivity, in the region which is similar to the results reported by Vagen *et al*. (2006). Field observations also showed that water level in those points is high. On the other hand, the effects of salt and sodium on the soil surface were also observed.

Because of all subscription and spectral characteristics of physical and chemical soil in these parts, another regression analysis was performed. The R-square for the remaining points were re-calculated and it was found that higher R-square values were obtained in relation to the general state when all of the data were considered. For example, R-square was 0.1 for band 3 for the whole data set while it was increased to 0.36 and 0.57 for the rest of the data set and the 40 series, respectively (Tables 3 and 4).

Therefore, the R-square value, which is statistically significant at the 5% level, is high only when the cation exchange capacity and digital values from combination bands are used. The highest R-square was derived for the 40 series when the original bands 1, 2, 3, the indices and the analysis of RI, SI, BI1, BI2, PD311, PD321, PCA3 and brightness components were applied. The highest R-square for the rest of points was derived when band 3, the indices and the analysis of PCA1, PD321, GEMI, VI5, BI1 and SI were applied in the regression equation.

The results showed that principal component analysis and regression models can be used to assess soil properties including cation exchange capacity. Fox and Metla (2005) also obtained similar results in Mid-West of the United States.

For the separated homogeneous data the regression coefficients increased considerably. R-square = 0.65 was obtained when the 40 series was applied, which shows a good correlation and dependency between the values. After separating the data series, it was observed that the residual data also showed higher R-square value. Figure 6 shows the scatter diagrams of cation exchange capacity obtained by the models for the 40 series and the rest of the data set.

As it can be seen in Fig. 7, most of the data values are located in the range of 95%. Band 3 and PD311 were used for series 1 and band 3 and PD321 were used for series 2 to estimate cation exchange in the study area. These data provide higher R-square and lower RMSE when the data applied in the regression analysis are taken from the area with homogenous characteristics. In this analysis it was found that after fitting the data Eq. (2) (R-square = 0.62 and RMSE = 2.87) and Eq. (3) (R-square = 0.47 and RMSE = 2.13) for series 1 and 2, respectively can be considered as appropriate models for estimating this variable.

T a b l e 2 . R-squares derived from regression between different vegetation indices and CEC applying the total data

Index	R^2	Index	R^2
Band 1	0.06000	Band 4	0.00300
Band 2	0.04000	Band 5	0.00800
Band 3	0.10000	Band 7	0.01000
PCA1	0.01000	Brightness	0.00200
PCA2	0.00800	Greenness	0.00050
PCA3	0.00300	Wetness	0.00006
PD322	0.04000	GEMI	0.00040
PD312	0.01000	MIRV1	0.00001
PD311	0.02700	MIRV2	0.00002
PD321	0.05000	VNIR1	0.00030
Stress-Related	0.00040	VNIR2	0.00050
Normalized-Based	0.00070	NDVI	0.00100
IPVI	0.00200	TVI	0.00100
OSAVI	0.00300	IR	0.00050
BI1	0.00800	IR2	0.00070
SI	0.00300	MND	0.00010
RI	0.00260	MINI	0.00070
MSAVI	0.00300	DVI	0.00020
BI2	0.00520	Complex Division2	0.00070
GVI	0.00080	Complex Division1	0.00030
VI1	0.00100	NDSI	0.00100
VI2	0.00003	EVI	0.00200
VI3	0.01000	G2	0.00040
VI4	0.00016	RA	0.00020
VI5	0.00230	SAVI	0.00200
VI6	0.00180	MIR	0.00022
VI7	0.00001	RVI	0.00001
VI8	0.00002	Complex Multiratio	0.00200
VI9	0.00002	Ratio-Based	0.00100
MSI	0.00040	COSRI	0.00100
MSR	0.00100	RATIO	0.00080

T a b l e 3. R-squares derived from regression between different vegetation indices and CEC applying the 273 remaining data

Index	R^2	Index	R^2
Band 1	0.2500	Band 4	0.0700
Band 2	0.2200	Band 5	0.1600
Band 3	0.3600	Band 7	0.1800
PCA1	0.3000	Brightness	0.2000
PCA2	0.2000	Greenness	0.2000
PCA3	0.2300	Wetness	0.1100
PD322	0.2000	GEMI	0.2600
PD312	0.1100	MIRV1	0.0200
PD311	0.2000	MIRV2	0.0400
PD321	0.3300	VNIR1	0.0300
Stress-Related	0.0400	VNIR2	0.0500
Normalized-Based	0.0700	NDVI	0.1000
IPVI	0.2000	TVI	0.1000
OSAVI	0.2000	IR	0.0500
BI1	0.2800	IR2	0.0700
SI	0.3000	MND	0.0100
RI	0.2400	MINI	0.0700
MSAVI	0.2000	DVI	0.0200
BI2	0.2500	Complex Division2	0.0800
GVI	0.0800	Complex Division1	0.0200
VI1	0.1000	NDSI	0.1000
VI2	0.0004	EVI	0.0200
VI3	0.0400	G2	0.1600
VI4	0.0100	RA	0.0200
VI5	0.2300	SAVI	0.2000
VI6	0.1400	MIR	0.1000
VI7	0.0100	RVI	0.1600
VI8	0.0200	Complex Multiratio	0.0400
VI9	0.0200	Ratio-Based	0.2000
MSI	0.0400	COSRI	0.1000
MSR	0.1000	RATIO	0.1000

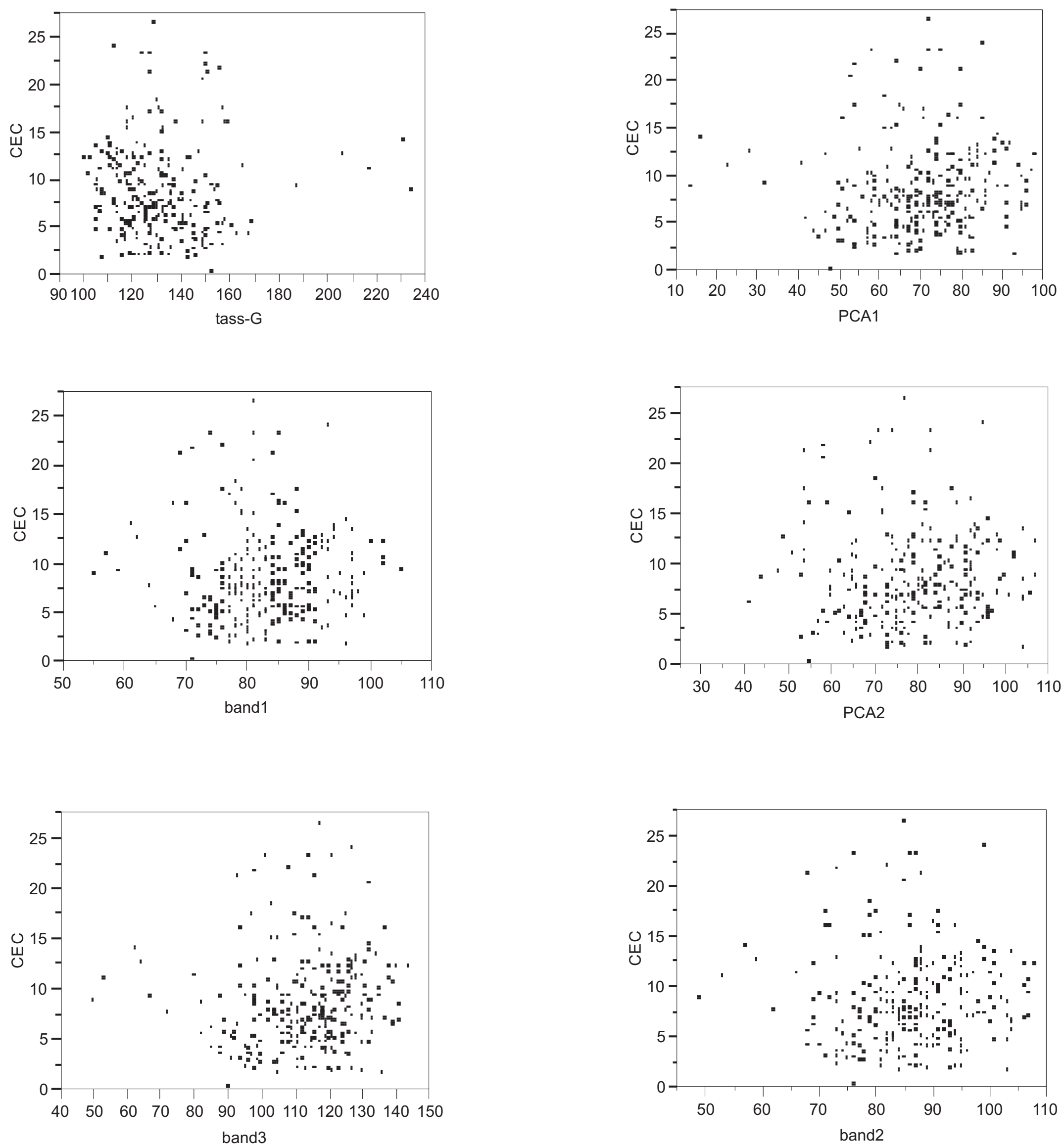

Fig. 3. Scatter diagram of soil cation exchange capacity against digital numbers in some of the analyses (when all the data set was used).

$$CEC= -8.05+0.37\ PD321+0.13\ b3 \quad (2)$$

$$CEC= 9.15 +0.24\ PD311+0.15\ b3 \quad (3)$$

Statistical analysis showed that PD321 and PD311 indices are more correlated with the amount of cation exchange capacity than other bands. It should be noted that band 1, 2 and 3 are involved in calculating both of the indices.

Therefore, experimental data with homogeneous characteristics have more effects on reflectance, so that the effect could be seen as a similar trend in all of the image processing used for monitoring of the changes in the region.

The above results are similar with the ones that Huete (1996) reported. This shows that the digital analysis of ETM^+ images can be used for evaluation of natural phenomena and land cover.

The results of spectral analysis showed that the total values of silt and clay in the segregated parts of the study area is high, which affected soil darkness and therefore resulted in more light absorption. Research in this field by White *et al*. (1997) showed that soils with high amounts of sand have almost no absorption in the visible and infrared band. Formaggio *et al*. (1996) also reported that the resulting reflectance bands from soils with higher CEC are much lower than other soils.

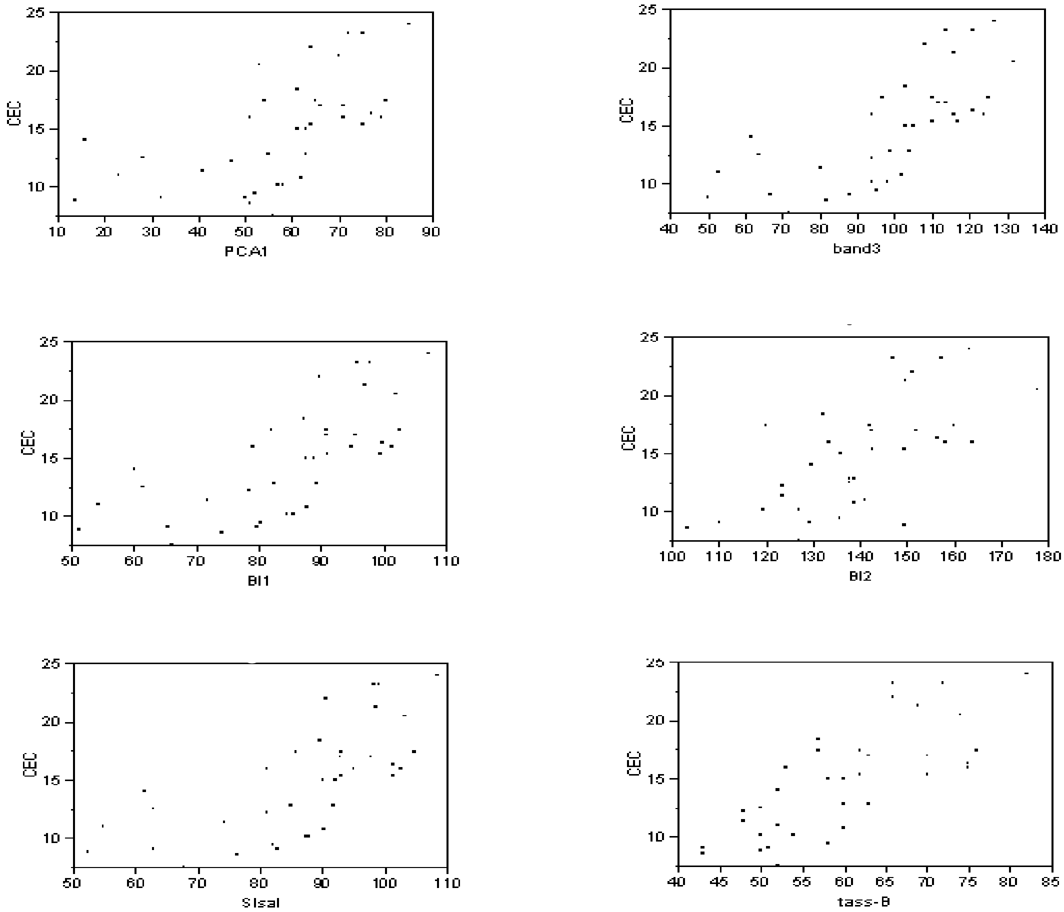

Fig. 4. Scatter diagram soil cation exchange capacity against digital numbers in some of the analyses (the 40 series was used).

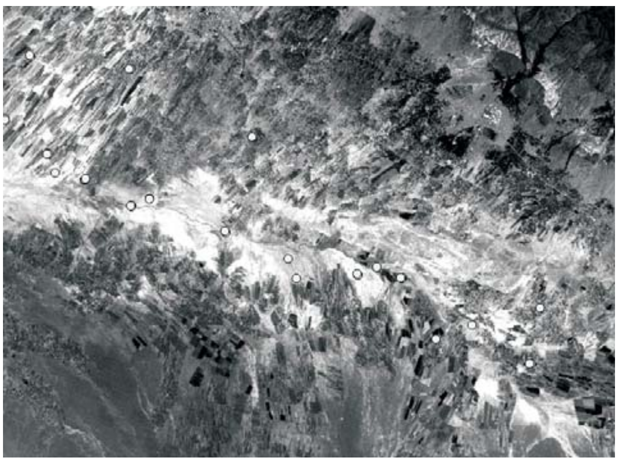

Fig. 5. Geographical positions of the 40 series data points with ETM^{+} image of the study area (in background).

CONCLUSIONS

1. Accordingly, the potential of remote sensing for soil variability in arid and semi-arid areas is limited because of special features of land cover and soils in those areas.

2. Using different image processing such as band ratios and principal component analysis increased R-squared values and provided better information than single band analysis. However, care must be taken in selecting appropriate methods according to the area features and the highest correlation coefficient.

3. The analysis of digital numbers showed that ETM^{+} images have a great potential for the evaluation of soil properties in areas with homogenous features.

4. The practical results can be used for applying proper management programs in the study area. It was also concluded that because of complexity in soil properties radiation signature it is hard to distinguish different soil properties by using only remote sensing data. Finally, this study showed that spatial analysis is essential for the study area because the soil properties are varied spatially very much.

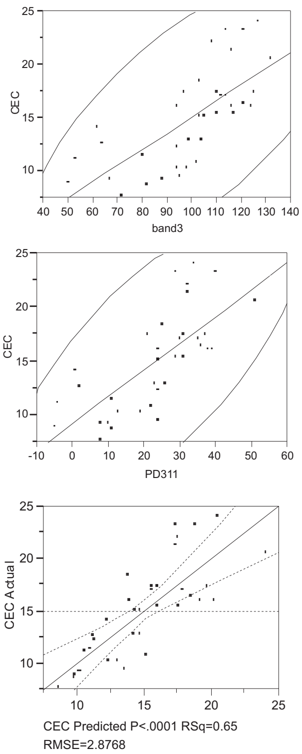

Fig. 6. Scatter diagram of soil cation exchange capacity against the image digital numbers when the 40 series data were applied.

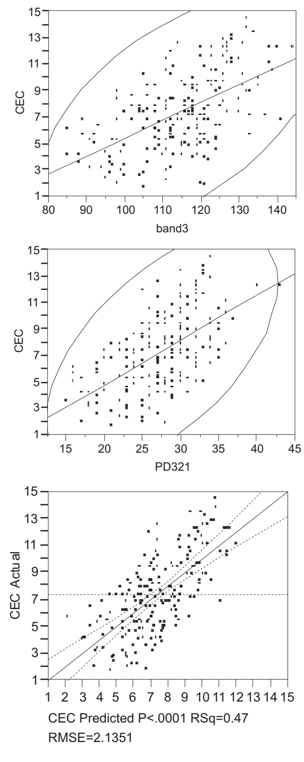

Fig. 7. Scatter diagram of soil cation exchange capacity against the image digital numbers when the remaining data were applied excluding the 40 series data.

T a b l e 4. R-squares derived from regression between different vegetation indices and CEC applying the 40 series data

Index	R^2	Index	R^2
Band 1	0.3700	Band 4	0.0040
Band 2	0.4400	Band 5	0.3200
Band 3	0.5700	Band 7	0.2400
PCA1	0.3500	Brightness	0.5000
PCA2	0.3400	Greenness	0.1500
PCA3	0.4200	Wetness	0.1700
PD322	0.3600	GEMI	0.1000
PD312	0.4300	MIRV1	0.0160
PD311	0.5100	MIRV2	0.2000
PD321	0.4700	VNIR1	0.0500
Stress-Related	0.0400	VNIR2	0.1000
Normalized-Based	0.0700	NDVI	0.2000
IPVI	0.2000	TVI	0.2000
OSAVI	0.2000	IR	0.1000
BI1	0.5000	IR2	0.0800
SI	0.4700	MND	0.2000
RI	0.5200	MINI	0.1000
MSAVI	0.2000	DVI	0.2100
BI2	0.4200	Complex Division2	0.1300
GVI	0.1200	Complex Division1	0.1400
VI1	0.2000	NDSI	0.2000
VI2	0.0600	EVI	0.0400
VI3	0.0004	G2	0.2000
VI4	0.2200	RA	0.1500
VI5	0.3100	SAVI	0.2000
VI6	0.1600	MIR	0.0500
VI7	0.0200	RVI	0.2000
VI8	0.2900	Complex Multiratio	0.2000
VI9	0.0100	Ratio-Based	0.1000
MSI	0.1100	COSRI	0.1500
MSR	0.2000	RATIO	0.2000

REFERENCES

Arzani H. and King G.W., 2008. Application of remote sensing (landsat TM data) for vegetation parameters measurement in western division of NSW. Int. Grassland Congr., 29 June – 5 July, Hohhot, China.

Bahtti A.U., Mulla D.J., and Frazier B.E., 1991. Estimation of soil properties and wheat yields on complex eroded hills using geostatistics and thematic mapper images. Remote sens. Environment, 31, 181-191.

Barnes E.M., Sudduth K.A., Hummel J.W., Lesch S.M., Corwin D.L., Yang C., Daughtry C.S.T., and Bausch W.C., 2003. Remote and ground-based sensore techniques to map soil properties. Photogrammetric Eng. Remote Sensing, 69(6), 619-630.

Batjes N.H., 2002. isric-wise global data set of derived soil properties on a 0.5 by degree grid (version 2). international soil reference and information center (ISRIC). Report, 2003/03 http:.\\www.isric.org), wageningen, 1-14

Chapman H.D., 1965. Cation exchange capacity. In: Black, C.A. etal. (eds.). Methods of Soil Analysis: Part 2. Monograph, Am. Soc. Agronomy, 9, 891-901.

Dematte J.A.M., Galodos M.V., Guimaraes R.V., Genu A.M., Nanins M.R., and Zullo J., 2007. Quantification of tropical soil attributes from ETM+ LANDSAT-7 data. Int. J. Remote Sensing, 17(28), 3813-3829.

Foody G.M., Cutler M., Mcmorrow J., Pelz D., Tangki H., Boyd D.S., and Douglas I., 2001. Mapping the biomass of Bornean tropical rain forest from remotely sensed data. J. Global Ecology Biogeography, 10, 379-387.

Formaggio A.R., Epiphanio J.C.N., Valeriano M.M., and Olivera J.B., 1996. Comportamento spectral (450-2.450 nm) de solos tropic is de Sao Paulo [Spectral (450-2450 nm) behavior of tropical soils from the State of Sao Paulo]. Revista Brasileira de Ciencia do Solo, 20, 467-474.

Fox G.A. and Metla R., 2005. Soil property analysis using principal components analysis, soil line and regression models. J. Soil Sci. Soc. Am., 69, 4782-1788.

Frazier B.E. and Cheng Y., 1989. Remote sensing of soils in eastern palouse region with landsat thematic mapper, Remote sense. Environment, 28, 317-325.

Gee G.W. and Bauder J.W., 1986. Particle-size analysis. In: Methods of Soil Analysis Part 1. Soil Science Society of America Book Series 5, Madison, WI, USA.

Huete A.R., 1996. Extension of soil spectra to the satellite: atmosphere, geometric and sensor considerations. Photo-interpretation, 34, 101-114.

Johannsen C.J., Carter P.G., Willis P.R., Owubah E., Erickson B., Ross K., and Targulian N., 1998. Applying remote sensing technology to precision farming. Proc. IV Int. Conf. Precision Agriculture, July 19-22, St. Paul, MN, USA.

Leblon B., 1993. Soil and vegetation optical properties. In: Applications in Remote Sensing, Volume 4, The International Center for Remote Sensing Education. Wiley Press, New York, USA.

Matinfar H.R., Sarmadian F., and Alavipanah S.K., 2011. Use of DEM and ASTER sensor data for soil and agricultural characterizing. Int. Agrophys., 25, 37-46.

Nikolakopoulos K.G., 2003. Use of vegetation indexes with ASTER VNIR data for burnt areas detection in Western Peloponnese, Greece. IEEE Int. Geoscience and Remote Sensing Symp., September 21-25, Toulouse, France.

Pettorelli N., Vik J.O., Mysterud A., Gaillard J.M., Tucker C.J., and Stenseth N.C., 2005. Using the satellite-derived NDVI to assess ecological responses to environmental change. J. Trends Ecology Evolution, 9(20), 503-510.

Phillips J.D., 1994. Deterministic uncertainty in landscapes Earth Surface proc. Landforms,19, 389-401.

Post D.F., Fimbres A., Matthiass A.D., Sano E.E., Accioly L., Batchily A.K., and Ferreira L.G., 2000. Predicting soil albedo from soil color and spectral reflectance data. Soil Sci. Soc. Am. J., 64(3), 1027-1034.

Vagen T.G., Shepherd K.D., and Walsh M.G., 2006. Sensing landscape level change in soil fertility following deforestation and conversion in the highlands of Madagascar using Vis-NIR spectroscopy. Geoderma, 133, 281-294.

Walkely A. and Black I.A., 1934. An examination of the Degtjareff method for determining soil organic matter and a proposed modification of the chromic acid titration method. Soil Sci., 37, 29-38.

White K., Walden J., Drake N., Eckardt F., and Settle J., 1997. Mapping the iron oxide content of dune sands, Namib Sand Sea, Namibia, using Landsat Thematic Mapper Data. Remote Sensing of Environment, 62, 30-39.